



## Molecular progression of SHH-activated medulloblastomas

Andrey Korshunov<sup>1,2,3</sup> · Konstantin Okonechnikov<sup>3,4</sup> · Felix Sahn<sup>1,2,3</sup> · Marina Ryzhova<sup>5</sup> · Damian Stichel<sup>1,2</sup> · Philipp Sievers<sup>1,2</sup> · Jochen Meyer<sup>1,2</sup> · Daniel Schrimpf<sup>1,2</sup> · Olga Zheludkova<sup>6</sup> · Andrey Golanov<sup>7</sup> · Peter Lichter<sup>3,8</sup> · David T. W. Jones<sup>3,4</sup> · Stefan M. Pfister<sup>3,4,9</sup> · Andreas von Deimling<sup>1,2,3</sup> · Marcel Kool<sup>3,4</sup>

Received: 1 April 2019 / Revised: 24 April 2019 / Accepted: 24 April 2019 / Published online: 27 April 2019  
© Springer-Verlag GmbH Germany, part of Springer Nature 2019

Medulloblastoma (MB) comprises four main molecular MB subgroups (WNT, SHH, Group 3 and Group 4) with divergent biology, outcomes and subgroup-specific differences in relapses [1–6]. Metastatic recurrences are most common in Group 3 and 4 MB, where metastases from a single patient are genetically similar to each other, but highly divergent from the corresponding primary tumor [2–6]. Local recurrences in the tumor bed are more frequent in SHH-activated tumors but progression-associated molecular aberrations for this MB variant remain unclear [2, 6]. To assess a biological evolution of SHH MB, we analyzed molecular changes appearing during local regrowth of desmoplastic nodular MB (DNMB). Eleven pairs of primary and recurrent DNMB samples were analyzed with DNA- and RNA-based methods. Tumor samples were obtained by resection from three infants, two children, and six adults older than 17 years (all at M0 stage; Suppl. Table). After primary resection, infants received chemotherapy alone, while children and adults were treated according to HIT protocols that included cranio-spinal radiotherapy as well. Event-free survival varied widely for these 11 patients, ranging from 8 to 192 months,

with infants on average relapsing earlier than non-infants (11 months vs. 82 months for others); all 11 “secondary” samples were obtained via resection of the local DNMB recurrences.

Histopathological evaluation revealed that eight DNMB pairs from children and adults had similar histology at primary diagnosis and at relapse. However, DNMB features completely disappeared in three infant recurrent samples which were represented by poorly differentiated, reticulin-rich areas (Fig. 1a, b). Methylation profiling disclosed matched DNA profiles for all DNMB pairs which all were identified as “SHH MB” according to “Classifier v11b4” [1] thus excluding secondary non-MB malignancies (Suppl. Figure 1). Cytogenetic profiles of eight children and adult DNMB revealed no detectable differences between primary and recurrent tumors (Table 1). In stark contrast, all three infant DNMB initially disclosed flat genomes, but their recurrences showed various CNVs including 17p loss in all three cases (Table 1, Fig. 1d). Next-generation panel sequencing (depth X900) revealed either *PTCH1* (8) or *SMO* (3) mutations; all three infants had both somatic and germ-line *PTCH1* alterations despite of balanced 9q (Table 1). *TERT* promoter mutations were identified in 4/6 adult DNMB. Mutational profiles were similar in eight pairs

**Electronic supplementary material** The online version of this article (<https://doi.org/10.1007/s00401-019-02022-y>) contains supplementary material, which is available to authorized users.

✉ Andrey Korshunov  
andrey.korshunov@med.uni-heidelberg.de

- 1 Clinical Cooperation Unit Neuropathology (G380), German Cancer Research Center (DKFZ) and German Cancer Consortium (DKTK), Im Neuenheimer Feld 280, 69120 Heidelberg, Germany
- 2 Department of Neuropathology, Heidelberg University Hospital, Heidelberg, Germany
- 3 Hopp Children’s Cancer Center at the NCT Heidelberg (KiTZ), Heidelberg, Germany
- 4 Division of Pediatric Neurooncology (B062), German Cancer Research Center (DKFZ) and German Cancer Consortium (DKTK), Heidelberg, Germany

- 5 Department of Neuropathology, NN Burdenko Neurosurgical Institute, Moscow, Russia
- 6 Department of Neuro-Oncology, Russian Scientific Center of Radiology, Moscow, Russia
- 7 Department of Neuroradiology, NN Burdenko Neurosurgical Institute, Moscow, Russia
- 8 Division of Molecular Genetics (B060), German Cancer Research Center (DKFZ) and German Cancer Consortium (DKTK), Heidelberg, Germany
- 9 Department of Pediatric Hematology and Oncology, Heidelberg University Hospital, Heidelberg, Germany

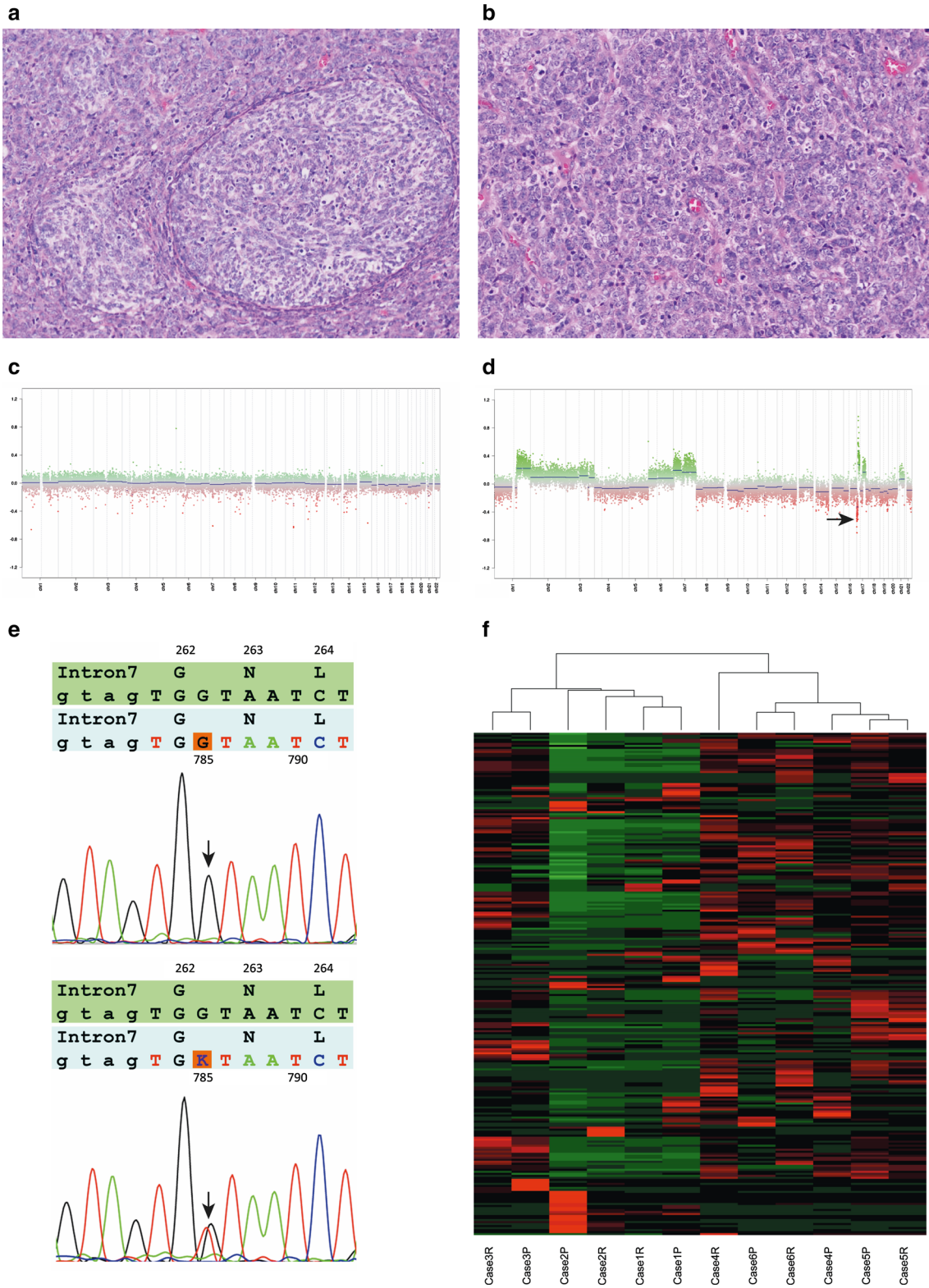


**Fig. 1** Primary and recurrent samples of DNMB in *PTCH1*-affected patients disclosed changes in histology and molecular profiles. **a** Typical DNMB appearance of primary tumor with “pale islands”. **b** Recurrent sample is represented by poorly differentiated, mitotically active tumor. **c** Primary infant DNMB (Case 1) disclosed flat genome, but recurrent sample (**d**) revealed numerous aberrations including 17p loss (arrow). **e** Primary infant tumor (Case 1; above) showed wt *TP53* (arrow) but recurrent sample (below) harbored *TP53* somatic mutation (p.G130V; arrow). **f** Gene expression-profiling data obtained after RNA sequencing of six paired DNMB samples. Heatmap of unsupervised hierarchical cluster analysis (based on top 500 high-variance genes) showed relative similarity of the transcriptional profiles generated for primary and recurrent DNMB with some expression differences, especially for infants (Cases 1 and 2)

of children/adults DNMB, although we cannot exclude a presence of alterations in genes not included in our panel. In contrast, all three recurrent infant DNMB disclosed somatic *TP53* mutations (Fig. 1e, Table 1) accompanied with intense *TP53* nuclear accumulation (not present in all primaries (Suppl. Figure 2)). RNA sequencing for six samples revealed a similarity of transcriptional profiles generated for DNMB pairs but with some differences in gene expression, especially for infants (Fig. 1f). In one recurrent DNMB harboring *TP53* mutation and 17p loss (Case 1), *TP53* expression level was significantly lower in comparison to primary sample thus suggesting its down-regulation due to a bi-allelic gene inactivation (Suppl. Figure 3).

The acquisition of various molecular events (including *TP53* mutations) has been described in relapsed SHH MB [2]. Here we discovered posttreatment DNMB molecular

aberrations in *PTCH1*-mutant infants which manifested as acquired CNVs and *TP53* mutations. However, due to a limited number of samples analyzed, these findings should be approved in representative series of relapsed SHH MB. Previously, *Ptch*-altered murine SHH MB showed *TP53* alterations as progression events [4, 7], although to draw any analogy between experimental and clinical data would be inappropriate. It is also unclear, whether these molecular changes are really progression-associated aberrations or they initially affect only a small population of the treatment-naïve, primary DNMB coming to the fore as a result of the posttreatment clonal selection. Somatic mutations in pediatric MB disclosed a spatial heterogeneity and, at time of relapse, major genetic divergences may occur between primary and recurrent tumors [4, 7]. Therefore, deep sequencing of multiregional tumor biopsies is an optimal way to detect genuine mutational landscape in *PTCH1*-affected patients.

The question of whether relapses in *PTCH1*-affected infants require a specific therapeutic approach warrants further consideration. Taking into account a presence of germline gene alterations, treatment intensification is still looking hazardous due to a risk of disease progression and secondary malignancies. Identified molecular aberrations could represent targets for MB salvage therapy, but their utility may be limited if they are not considered in the recurrent disease. Therefore, we could recommend a molecular analysis of the primary and recurrent DNMB samples synchronously because progression-associated aberrations may be taken

**Table 1** Molecular characteristics of primary and recurrent DNMB

N	CNVs primary	CNVs recurrent	Mutations primary	Mutation germ-line	Mutations recurrent
1	Balanced	+1q, +2, +6, +7, -17p, +17q	<i>PTCH1</i> (L1109fs/G1097fs/L1023I; 88%; 72%; 79% <sup>a</sup> )	<i>PTCH1</i> (L1109fs/L1023I; 49%; 48% <sup>a</sup> )	<i>PTCH1</i> (L1109fs/G1097fs/L1023I; 42%; 41%; 41% <sup>a</sup> ); <b><i>TP53</i> (G130V; 52%<sup>a</sup>)</b>
2	Balanced	-10q, +15q, -17p	<i>PTCH1</i> (A385fs/P1164L; 88%; 89% <sup>a</sup> )	<i>PTCH1</i> (A385fs; 48% <sup>a</sup> )	<i>PTCH1</i> (A385fs/P1164L; 71%; 68% <sup>a</sup> ); <b><i>TP53</i> (E126D; 75%<sup>a</sup>)</b>
3	Balanced	+2, -3p, +3q, +5p, -5q, -17p;	<i>PTCH1</i> (A300fs; 92% <sup>a</sup> )	<i>PTCH1</i> (A300fs; 47% <sup>a</sup> )	<i>PTCH1</i> (A385fs; 87% <sup>a</sup> ); <b><i>TP53</i> (M114K; 90%<sup>a</sup>)</b>
4	+1q, +2p, -2q, -4q, -9q, -17p	+1q, +2p, -2q, -4q, -9q, -17p	<i>PTCH1</i> (T858fs; 89% <sup>a</sup> )	No	<i>PTCH1</i> (T858fs; 86% <sup>a</sup> )
5	Balanced	Balanced	<i>SMO</i> (D473 N; 45% <sup>a</sup> )	No	<i>SMO</i> (D473N; 43% <sup>a</sup> )
6	-9q	-9q	<i>PTCH1</i> (S493fs; 82% <sup>a</sup> )	No	<i>PTCH1</i> (S493fs; 82% <sup>a</sup> )
7	+1q, +2, +3, +7, -16q	+1q, +2, +3, +7, -16q	<i>SMO</i> (S278I; 43% <sup>a</sup> )	No	<i>SMO</i> (S278I; 38% <sup>a</sup> )
8	Balanced	Balanced	<i>SMO</i> (L412F; 46% <sup>a</sup> )	No	<i>SMO</i> (L412F; 41% <sup>a</sup> )
9	-9q, -10q, -14q, -18q	-9q, -10q, -14q, -18q	<i>PTCH1</i> (G988fs; 77% <sup>a</sup> )	No	<i>PTCH1</i> (G988fs; 74% <sup>a</sup> )
10	-9q	-9q	<i>PTCH1</i> (N31fs; 78% <sup>a</sup> )	No	<i>PTCH1</i> (N31fs; 76% <sup>a</sup> )
11	+3q, -9q, -16q	+3q, -9q, -16q	<i>PTCH1</i> (C225fs; 81% <sup>a</sup> )	No	<i>PTCH1</i> (C225fs; 74% <sup>a</sup> )

*TP53*-associated acquired molecular aberrations are marked in bold

<sup>a</sup>Allele frequency

into service to making appropriate changes in the treatment strategy.

**Acknowledgements** A. Korshunov is supported by the Helmholtz Association Research Grant (Germany). M. Ryzhova, A. Golanov, and O. Zheludkova are supported by the RSF Research Grant no. 18-45-06012.

## References

1. Capper D, Stichel D, Sahm F, Jones DTW, Schrimpf D, Sill M et al (2018) Practical implementation of DNA methylation and copy-number-based CNS tumor diagnostics: the Heidelberg experience. *Acta Neuropathol* 136:181–210. <https://doi.org/10.1007/s00401-018-1879-y>
2. Hill RM, Kuijper S, Lindsey JC, Petrie K, Schwalbe EC, Barker K et al (2015) Combined MYC and P53 defects emerge at medulloblastoma relapse and define rapidly progressive, therapeutically targetable disease. *Cancer Cell* 27:72–84. <https://doi.org/10.1016/j.ccell.2014.11.002>
3. Kool M, Jones DT, Jäger N, Northcott PA, Pugh TJ, Hovestadt V et al (2014) Genome sequencing of SHH medulloblastoma predicts genotype-related response to smoothened inhibition. *Cancer Cell* 25:393–405. <https://doi.org/10.1016/j.ccr.2014.02.004>
4. Morrissy AS, Garzia L, Shih DJ, Zuyderduyn S, Huang X, Skowron P et al (2016) Divergent clonal selection dominates medulloblastoma at recurrence. *Nature* 529:351–357. <https://doi.org/10.1038/nature16478>
5. Northcott PA, Buchhalter I, Morrissy AS, Hovestadt V, Weischenfeldt J, Ehrenberger T et al (2017) The whole-genome landscape of medulloblastoma subtypes. *Nature* 547:311–317. <https://doi.org/10.1038/nature22973>
6. Ramaswamy V, Remke M, Bouffet E, Faria CC, Perreault S, Cho YJ et al (2013) Recurrence patterns across medulloblastoma subgroups: an integrated clinical and molecular analysis. *Lancet Oncol* 14:1200–1207. [https://doi.org/10.1016/S1473-2045\(13\)70449-2](https://doi.org/10.1016/S1473-2045(13)70449-2)
7. Tamayo-Orrigo L, Wu CL, Bouchard N, Khedher A, Swikert SM, Remke M et al (2016) Evasion of cell senescence leads to medulloblastoma progression. *Cell Rep* 14:2925–2937. <https://doi.org/10.1016/j.celrep.2016.02.061>

**Publisher's Note** Springer Nature remains neutral with regard to jurisdictional claims in published maps and institutional affiliations.